BIOCHEMISTRY
including biophysical chemistry & molecular biology

Article

pubs.acs.org/biochemistry

Nuclear Resonance Vibrational Spectroscopy and Electron Paramagnetic Resonance Spectroscopy of ^{57}Fe-Enriched [FeFe] Hydrogenase Indicate Stepwise Assembly of the H-Cluster

Jon M. Kuchenreuther,[†,‡] Yisong Guo,[§,∞] Hongxin Wang,[†,∥] William K. Myers,[†] Simon J. George,[†] Christine A. Boyke,[⊥] Yoshitaka Yoda,[@] E. Ercan Alp,[#] Jiyong Zhao,[#] R. David Britt,[†] James R. Swartz,[‡,▽] and Stephen P. Cramer*[,†,∥]

[†]Department of Chemistry, University of California, Davis, California 95616, United States
[‡]Department of Chemical Engineering, Stanford University, Stanford, California 94305, United States
[§]Department of Applied Science, University of California, Davis, California 95616, United States
[∥]Physical Biosciences Division, Lawrence Berkeley National Laboratory, Berkeley, California 94720, United States
[⊥]Department of Chemistry, University of Illinois at Urbana-Champaign, Urbana, Illinois 61801, United States
[@]JASRI, SPring-8, 1-1-1 Kouto, Sayo-cho, Sayo-gun, Hyogo 679-5198, Japan
[#]Advanced Photon Source, Argonne National Laboratory, Argonne, Illinois 60439, United States
[▽]Department of Bioengineering, Stanford University, Stanford, California 94305, United States

Supporting Information

ABSTRACT: The [FeFe] hydrogenase from *Clostridium pasteurianum* (CpI) harbors four Fe−S clusters that facilitate the transfer of an electron to the H-cluster, a ligand-coordinated six-iron prosthetic group that catalyzes the redox interconversion of protons and H_2. Here, we have used ^{57}Fe nuclear resonance vibrational spectroscopy (NRVS) to study the iron centers in CpI, and we compare our data to that for a [4Fe-4S] ferredoxin as well as a model complex resembling the $[2Fe]_H$ catalytic domain of the H-cluster. To enrich the hydrogenase with ^{57}Fe nuclei, we used cell-free methods to post-translationally mature the enzyme. Specifically, inactive CpI apoprotein with ^{56}Fe-labeled Fe−S clusters was activated *in vitro* using ^{57}Fe-enriched maturation proteins. This approach enabled us to selectively label the $[2Fe]_H$ subcluster with ^{57}Fe, which NRVS confirms by detecting ^{57}Fe−CO and ^{57}Fe−CN normal modes from the H-cluster nonprotein ligands. The NRVS and iron quantification results also suggest that the hydrogenase contains a second ^{57}Fe−S cluster. Electron paramagnetic resonance (EPR) spectroscopy indicates that this ^{57}Fe-enriched metal center is not the $[4Fe\text{-}4S]_H$ subcluster of the H-cluster. This finding demonstrates that the CpI hydrogenase retained an ^{56}Fe-enriched $[4Fe\text{-}4S]_H$ cluster during *in vitro* maturation, providing unambiguous evidence of stepwise assembly of the H-cluster. In addition, this work represents the first NRVS characterization of [FeFe] hydrogenases.

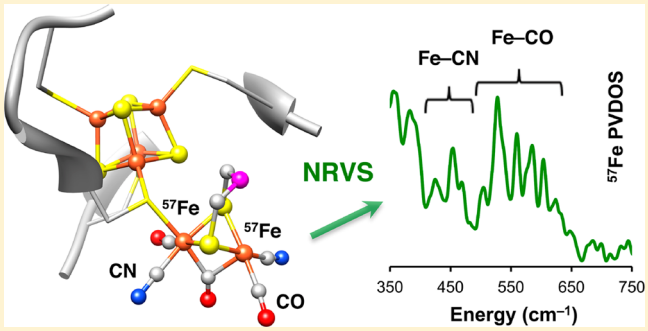

Hydrogenases are metalloproteins that have unique iron-based cofactors capable of catalyzing the redox interconversion of H_2 and protons. These enzymes have attracted interest not only for elucidating microbial evolution and physiology[1−3] but also for engineering renewable H_2 production technologies.[4,5] Furthermore, hydrogenases are appealing for their potential application as enzymes themselves[6,7] and as inspirational targets for the design of biomimetic H_2 catalysts.[8,9]

In the class of [FeFe] hydrogenases, the H_2 redox chemistry occurs at the H-cluster. As shown in Figure 1, the H-cluster is located within the H-domain of the enzyme, and it consists of a catalytic [FeFe] subunit (termed $[2Fe]_H$) linked via a cysteine ligand to a [4Fe-4S] cluster (termed $[4Fe\text{-}4S]_H$).[10,11] The $[2Fe]_H$ subcluster has multiple CO and CN^- nonprotein ligands as well as a bridging dithiolate substituent (DTMX). Most [FeFe] hydrogenases also have ancillary Fe−S clusters that are involved in the transfer of an electron to and from the H-cluster.[12] In the particular case of the monomeric HydA hydrogenase from *Clostridium pasteurianum*, commonly termed CpI, the F-domain electron transport chain consists of three [4Fe-4S] clusters as well as a [2Fe-2S] cluster (Figure 1).[11]

Unlike [4Fe-4S] and [2Fe-2S] clusters that are generally synthesized by host cell iron−sulfur cluster machinery, the $[2Fe]_H$ subcluster is made by three Fe−S accessory proteins called HydE,

Received: September 30, 2012
Revised: December 10, 2012
Published: December 18, 2012

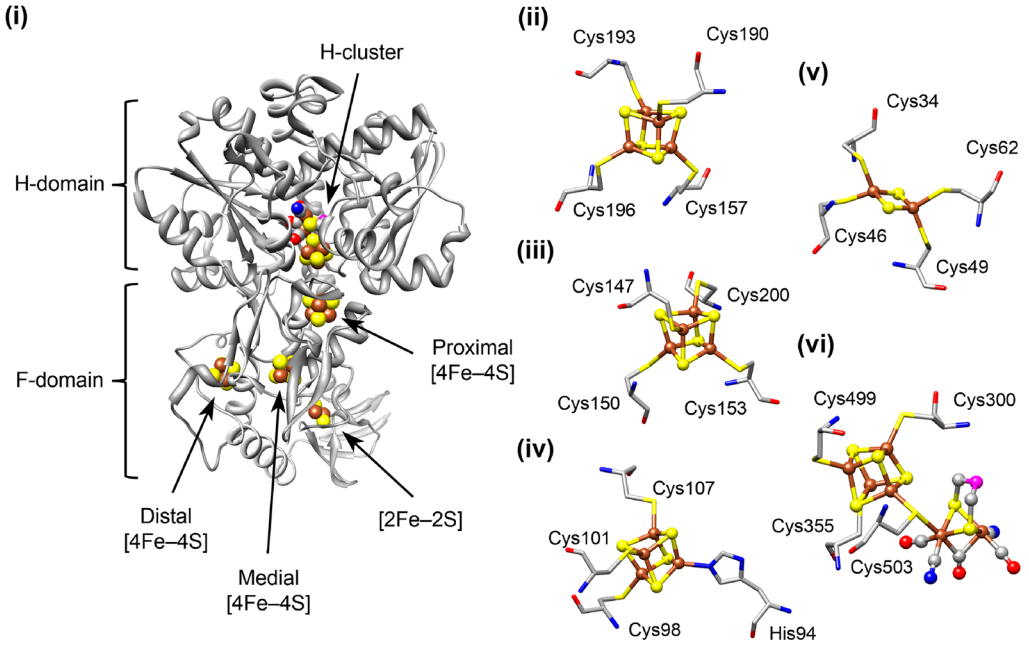

Figure 1. Structures of the iron cluster sites in the *C. pasteurianum* HydA hydrogenase (CpI). (i) Crystal structure of the CpI holoenzyme (Protein Data Bank entry 3C8Y) depicting the overall view of the electron transport chain within the F-domain. (ii) Proximal [4Fe-4S] accessory cluster. (iii) Medial [4Fe-4S] accessory cluster. (iv) Distal [4Fe-4S] accessory cluster, which is coordinated by three cysteine ligands and one histidine ligand. (v) [2Fe-2S] ferredoxin-like cluster. (vi) Active site H-cluster metal center, which consists of the $[4Fe\text{-}4S]_H$ subcluster joined to the $[2Fe]_H$ subcluster via the Cys503 residue. The H-cluster is shown in the H_{red} state with an open site at the distal Fe nucleus. Nonprotein ligands coordinated to the $[2Fe]_H$ subcluster include three CO molecules, two CN^- molecules, and a dithiol bridging molecule (DTMX) with an unknown central atom presumed to be either oxygen or nitrogen. Fe (brown), S (yellow), C (gray), O (red), N (blue), and an unknown atom (magenta) are shown. Molecular graphics were generated using UCSF Chimera.[56]

HydF, and HydG.[12,13] Currently, it is not entirely understood how the $[2Fe]_H$ subcluster is assembled by these three Hyd maturases. Recent reports have shed light on the biosynthetic reaction sequence, mainly from *in vitro* studies focusing on characterizing the biochemistry of the Hyd proteins.[14−17] For example, it has been suggested that HydF transfers the $[2Fe]_H$ subcluster to the $[4Fe\text{-}4S]_H$-containing hydrogenase apoprotein, thus producing the active enzyme.[18]

Equally important to unraveling how the H-cluster is assembled will be to understand its structural and electronic transformations among the different redox configurations, which is crucial for establishing the catalytic cycle of the H-cluster. [FeFe] hydrogenases have been extensively characterized by X-ray crystallography and various advanced spectroscopies, and at least seven different H-cluster substates have been observed.[19−21] Quantum and molecular mechanics (QM/MM) calculations combined with density functional theory (DFT) have provided further insights into the catalytic cycle between various redox configurations such as the oxidized (H_{ox}) and reduced (H_{red}) states,[22] yet it has been challenging for researchers to develop synthetic catalysts that function like and as effectively as [FeFe] hydrogenases, due in part to a poor mechanistic understanding of how the H-cluster evolves H_2.[9] Certainly, elucidating the biosynthetic pathway of the H-cluster and developing functional biomimetic catalysts are areas of active research that would benefit from new approaches to studying [FeFe] hydrogenases.[12,15,23]

Nuclear resonance vibrational spectroscopy (NRVS) is an exciting and novel approach for investigating the vibrational dynamics of Fe in metalloproteins.[24−26] The fundamental physics of NRVS have been described in detail elsewhere.[27−30] Measurements involve scanning an extremely monochromatic (<1 meV) X-ray beam through a nuclear resonance and recording the vibrational information associated with an ^{57}Fe nuclear transition via the subsequent Fe K_α emission. While the resulting spectrum is similar to an infrared (IR) or resonance Raman (RR) spectrum,[31] different intensity mechanisms apply. Specifically, the NRVS intensity for a particular normal mode is related to the movement of the resonant nucleus (in this case, ^{57}Fe) along the direction of the incident X-ray beam,[30,32] and results are generally reported as an ^{57}Fe-centered partial vibrational density of states (PVDOS).[32−34] With its particular elemental and isotopic specificity, NRVS provides a valuable complement to more conventional spectroscopies. Unlike IR spectroscopy, NRVS does not incur interference from water or protein-based modes. In contrast to RR spectroscopy, NRVS can probe any oxidation state and is impervious to sample fluorescence.

In this work, we present the results of NRVS of the CpI hydrogenase selectively enriched with ^{57}Fe, which we term $CpI^{[^{57}Fe]H}$. To produce the $CpI^{[^{57}Fe]H}$ hydrogenase, a cell-free approach was used to post-translationally mature the apoenzyme. The inactive apoprotein was first expressed in *Escherichia coli* grown in ^{56}Fe-supplemented medium, and the hydrogenase was then activated *in vitro* using ^{57}Fe-enriched Hyd maturases. NRVS confirms the incorporation of ^{57}Fe nuclei into the $CpI^{[^{57}Fe]H}$ holoenzyme, and we compare our results to NRVS data for a model complex inspired by the $[2Fe]_H$ subcluster. In doing so, we observe the presence of $^{57}Fe{-}CO$ and $^{57}Fe{-}CN$ normal modes. The NRVS data also show that a second Fe−S cluster contains ^{57}Fe nuclei. However, EPR spectroscopy indicates that this iron center is not the $[4Fe\text{-}4S]_H$ subcluster.

MATERIALS AND METHODS

Preparation of Aqueous ^{57}Fe. All steps were performed in a fume hood. Solutions were constantly stirred and chilled using ice baths. To prepare ~80 mL of 65 mM ^{57}Fe (final pH of ~1),

dx.doi.org/10.1021/bi301336r | *Biochemistry* 2013, 52, 818−826

metallic ^{57}Fe was dissolved using *aqua regia*. First, 5 mL of nitric acid (>65%) was added to 300 mg of metallic ^{57}Fe in a 150 mL glass beaker. Next, 12 mL of 12 M hydrochloric acid was added dropwise. After the ^{57}Fe was completely dissolved, 40 mL of 5 M sodium hydroxide was slowly added for partial neutralization, followed by 15 mL of 1.5 M sodium citrate and 15 mL of 1 M ammonium hydroxide.

***In Vitro* Preparation of ^{57}Fe-Enriched [FeFe] Hydrogenase for NRVS.** Both the CpI apoprotein and the *Shewanella oneidensis* HydE, HydF, and HydG maturases were anaerobically produced in *E. coli* strain BL21(DE3) Δ*iscR::kan* using methods previously described for high-yield production of metalloproteins that contain stoichiometric amounts of Fe−S clusters.[15,35] Inactive CpI-*Strep*-tag II apoprotein was produced in *E. coli* grown in complex medium with natural abundance Fe (250 mg/L ferric ammonium citrate). HydE, HydF, and HydG were separately expressed in *E. coli* grown in complex medium supplemented with 200 μM ^{57}Fe instead of natural abundance Fe. By using a colorimetric assay described by Fish,[36] we estimated that the growth medium prepared from commercial LB Broth Miller (EMD Chemicals) contained <2 μM natural abundance Fe. Each maturase was individually expressed in *E. coli* to prevent the in vivo assembly of a HydF-bound $[2Fe]_H$ precursor that results when HydF is co-expressed with HydE and HydG.[17,37] Cell lysates with the ^{57}Fe-enriched maturases (HydE$^{[57Fe]}$, HydF$^{[57Fe]}$, and HydG$^{[57Fe]}$) were prepared using BugBuster Master Mix lysis solution (4 mL per gram of wet cell paste) supplemented with 100 mM HEPES (pH 8.2).

The CpI enzyme was post-translationally activated using previously described methods for cell-free synthesis of the H-cluster and hydrogenase maturation.[15] In general terms, the in vitro maturation reaction mixture is a combination of inactive CpI apoprotein, extrinsic low-molecular weight substrates, and three *E. coli* lysates containing the HydE, HydF, and HydG maturases. Specifically, *in vitro* CpI maturation reaction mixtures (60 mL) contained 3 mL of HydE$^{[57Fe]}$ lysate, 10 mL of HydF$^{[57Fe]}$ lysate, 30 mL of HydG$^{[57Fe]}$ lysate, 1 mM aqueous ^{57}Fe as described above, 1 mM sodium sulfide, 1 mM DTT, 2 mM *S*-adenosylmethionine, 2 mM L-cysteine, 2 mM L-tyrosine, 15 mM GTP, 1 mM pyridoxal 5′-phosphate, 2 mM sodium dithionite, and 300 mg/L purified and desalted CpI apoenzyme (5 μM). After anaerobic incubation for 24 h at 23 °C, reaction mixtures were clarified at 20000*g* for 10 min to remove precipitate that formed during the reaction. Prior to the purification step, the pH of the clarified reaction mixture was adjusted to 7.5 using 1 M HEPES buffer (pH 8.2). Active CpI was isolated using *Strep*-Tactin Superflow high-capacity resin (IBA GmbH), and the purified holoenzyme was concentrated to 25−50 μM using a stirred cell with a 5 kDa membrane (Amicon). Active CpI was further concentrated to ∼3 mM and a final volume of 75 μL using 30 kDa centrifugal filters (Amicon). The concentrated CpI$^{[57Fe]H}$ was loaded into 3 mm × 7 mm × 1 mm (interior dimensions) Lucite cuvettes and stored in liquid N_2.

Biochemical Characterization of CpI$^{[57Fe]H}$. CpI specific activities were measured using a methyl viologen activity assay.[15] Protein concentrations were determined using the Bradford method[38] along with a conversion factor specific to the CpI enzyme for dye-based assays.[39] A ferrozine-based colorimetric assay was used to measure iron content.[36]

NRVS Measurements. NRVS measurements were recorded using previously described methods.[30] The raw NRVS data were analyzed with PHOENIX[40] to extract the single-phonon ^{57}Fe-centered partial vibrational densities of states (PVDOS). Each ^{57}Fe PVDOS spectrum represents the average of the total number of scans, which was determined by adding scans and normalizing to the intensity of the incident beam.

The CpI$^{[57Fe]H}$ samples were measured at beamline 09-XU at SPring-8 (energy resolution of ∼0.8 meV, beam flux of ∼1.4 × 10^9 photons/s).[41] During NRVS measurements, samples were maintained at low temperatures using a liquid He cryostat. Actual temperatures for the CpI$^{[57Fe]H}$ samples were ∼50 K as obtained from the spectral imbalance analysis. Delayed nuclear fluorescence and Fe K_α fluorescence (from internal conversion) emitted by ^{57}Fe atoms were recorded with a four-channel avalanche photodiode (APD) array. Scans took 45−60 min (varying from scan to scan), and measurements were taken with 0.27 meV steps. Scans of the CpI$^{[57Fe]H}$ samples were separated into multiple sections, and different scan times were used for each section. Specifically, points were measured for 1−3 s between 0 and 350 cm^{-1} and for 10−25 s between 350 and 800 cm^{-1}. The resonant peak intensity for the CpI$^{[57Fe]H}$ measurements was 340 counts/s.

The $[^{57}Fe_2(S_2C_3H_6)(CN)_2(CO)_4]^{2-}$ model complexes were measured at beamline 3-ID at the Advanced Photon Source (APS) (resolution of ∼1.0 meV, beam flux of ∼3.2 × 10^9 photons/s).[42] The samples were measured at low temperatures using a similar liquid helium cryostat. The packed and sealed powder samples were mounted onto the cryostat base with two to four screws. Actual sample temperatures were ∼75 K as obtained from the spectral imbalance analysis. The Fe emission was recorded with a single 1 cm^2 square APD, and measurements were taken with ∼0.25 meV steps. The resonance peak intensities were 1100 and 1700 counts/s for the natural abundance CN and ^{13}CN-labeled model compounds, respectively.

EPR Spectroscopy. EPR measurements were performed at the CalEPR Center in the Department of Chemistry at the University of California (Davis, CA). Continuous-wave (CW) spectra were collected at an X-band frequency (9.39 GHz) with either a Bruker Biospin ECS106 spectrometer or a Bruker Biospin Elexsys E500 spectrometer equipped with a cylindrical TE_{011}-mode resonator (SHQE-W), an ESR-900 liquid helium cryostat, and an ITC-5 temperature controller (Oxford Instruments). Unless otherwise noted, measurement parameters were as follows: 15 K, 62 μW microwave power, 0.5 mT modulation amplitude, 81.9 ms time constant, and 81.9 ms conversion time. Intensities were normalized to the temperature, time constant, receiver gain, number of scans, modulation amplitude, and square root of the microwave power. Simulations were performed using MatLab and EasySpin.[43]

RESULTS

***In Vitro* Activation of the CpI$^{[57Fe]H}$ Hydrogenase.** Two independent CpI$^{[57Fe]H}$ samples were prepared from separate cell-free maturation reaction mixtures that contained exogenous substrates, including ^{57}Fe, non-purified ^{57}Fe-enriched Hyd maturases, and ^{56}Fe-enriched CpI apoprotein. It is currently unclear which maturase harbors the Fe cluster onto which the CO, CN^-, and DTMX ligands are coordinated. One hypothesis for $[2Fe]_H$ subcluster assembly involves the transfer of HydG-derived CO and CN^- molecules to a HydF-bound [2Fe-2S] scaffold cluster.[44] A second hypothesis states that HydG synthesizes an iron compound precursor with ligated CO and CN^- that is shuttled to the hydrogenase via HydF.[14] However, neither reaction

dx.doi.org/10.1021/bi301336r | *Biochemistry* 2013, 52, 818−826

sequence has been experimentally demonstrated. Therefore, all three maturases used in this study were enriched with ^{57}Fe by producing them with growth medium supplemented with exogenous ^{57}Fe.

Both the biochemical characterization and the measured NRVS spectra were similar for the two CpI$^{[^{57}Fe]H}$ samples (Supporting Information, Figure S4). On the basis of activity measurements [558 ± 43 μmol of H_2 consumed min^{-1} (mg of CpI)$^{-1}$], we estimated that 85% of the CpI apoprotein was activated during the *in vitro* reaction. Roughly 80% of the active enzyme was recovered during the purification step and prepared for NRVS measurements (3 mM CpI$^{[^{57}Fe]H}$). Iron quantification data from a ferrozine-based colorimetric assay indicate that the CpI apoenzyme and CpI$^{[^{57}Fe]H}$ holoenzyme contained 12.7 ± 2.4 and 17.5 ± 1.7 total Fe atoms per protein, respectively.

NRVS. In Figure 2, the ^{57}Fe PVDOS from 0 to 450 cm^{-1} for CpI$^{[^{57}Fe]H}$ is compared to previously reported data for an

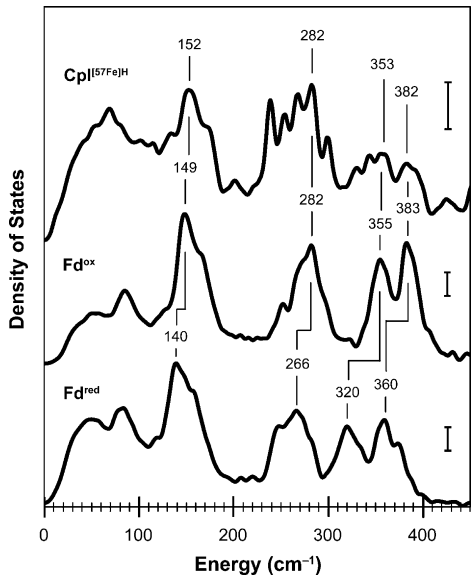

Figure 2. NRVS data within the 0–450 cm^{-1} range of energies for the CpI$^{[^{57}Fe]H}$ hydrogenase and the *Pf* D14C [4Fe-4S] ferredoxin (Fd). The ^{57}Fe vibrational densities of states are shown for CpI$^{[^{57}Fe]H}$ (59 scans; top curve) and previously published data by Mitra and co-workers for both oxidized Fd (middle curve) and reduced Fd (bottom curve).[25] Energies for selected Fe–S vibrational modes are indicated, and vertical scale bars represent 30 cm for the ^{57}Fe PVDOS.

^{57}Fe-enriched mutant of the *Pyrococcus furiosus* [4Fe-4S] ferredoxin (the *Pf* D14C Fd variant).[25] Within this region, the main features include large-scale protein movements and Fe–S cluster torsional modes below 100 cm^{-1}, strong Fe–S bending and breathing modes from 100 to 200 cm^{-1}, and bands characteristic of Fe–S stretching modes [ν(FeS)] from 200 to 400 cm^{-1}. The similar peak positions and line shapes between the ^{57}Fe vibrational density of states for the CpI$^{[^{57}Fe]H}$ hydrogenase and the oxidized *Pf* D14C Fd indicate the presence of an ^{57}Fe-labeled [4Fe-4S]$^{2+}$ cluster in the hydrogenase. Among the useful indicators, oxidized [4Fe-4S]$^{2+}$ clusters have ν(FeS) stretches near 282, 355, and 383 cm^{-1},[25] and similar strong bands were observed for the CpI$^{[^{57}Fe]H}$ hydrogenase. In addition, the CpI spectrum shows an intense Fe bending mode around 150 cm^{-1} as well as ν(FeS) stretching modes between 230 and 290 cm^{-1} that are noticeably absent in a previously reported NRVS study of the *Rhodobacter capsulatus* [2Fe-2S] ferredoxin,[45] which supports our assignment of these peaks to an ^{57}Fe-enriched [4Fe-4S] cluster.

The higher-energy region of the NRVS spectrum is more chemically interesting because this region is where vibrational modes from the Fe–CO and Fe–CN moieties associated with the [FeFe] hydrogenase $[2Fe]_H$ subcluster should arise. Figure 3

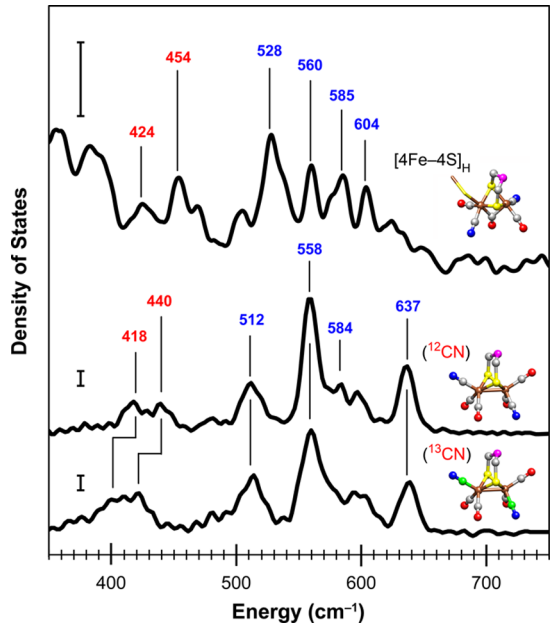

Figure 3. NRVS data within the 350–750 cm^{-1} range of energies for the CpI$^{[^{57}Fe]H}$ hydrogenase and the $[^{57}Fe_2(S_2C_3H_6)(CN)_2(CO)_4]^{2-}$ model complex. The ^{57}Fe vibrational densities of states are shown for CpI$^{[^{57}Fe]H}$ (59 scans; top curve) as well as the model compound containing either CN^- ligands (five scans; middle curve) or isotopically labeled $^{13}CN^-$ ligands (five scans; bottom curve). Selected energies are indicated for Fe–CN modes (red labels) and Fe–CO modes (blue labels). The vertical scale bars represent 30 cm for the ^{57}Fe PVDOS. Structures are shown for the $[2Fe]_H$ subcluster (Protein Data Bank entry 3C8Y) and the model complex (CCDC entry ODEDUW) with the following color scheme: brown for Fe, yellow for S, gray for C, green for ^{13}C, red for O, blue for N, and magenta for unknown. Molecular graphics were generated using UCSF Chimera.[56]

presents the spectrum for CpI$^{[^{57}Fe]H}$ from 350 to 750 cm^{-1} and compares it to two NRVS spectra from the $[^{57}Fe_2(S_2C_3H_6)(CN)_2(CO)_4]^{2-}$ model compound that has either CN^- or $^{13}CN^-$ ligands. Our Fe–CO and Fe–CN mode assignments for the CpI$^{[^{57}Fe]H}$ hydrogenase are based on prior NRVS of the iron–sulfur cluster-free hydrogenase (Hmd)[24] as well as our NRVS results from the model complex. To assign the Fe–CO and Fe–CN vibrations for the model compound, we performed both DFT calculations and FTIR spectroscopy in the far-IR region (300–700 cm^{-1}) and the mid-IR region (1700–2200 cm^{-1}), and a more detailed analysis of the model complex is provided in the Supporting Information.

In the NRVS spectrum for the $[^{57}Fe_2(S_2C_3H_6)(CN)_2(CO)_4]^{2-}$ model compound, two peaks at 418 and 440 cm^{-1} are shown within the 375–500 cm^{-1} region, which shift downward ~18 cm^{-1} upon ^{13}CN substitution. We assign these features as mainly the combination of Fe–CN stretching modes [ν(Fe–CN)] and

dx.doi.org/10.1021/bi301336r | *Biochemistry* 2013, 52, 818–826

Fe−CN bending modes [δ(Fe−CN)]. In the 500−700 cm^{-1} region, the model compound exhibits a complex vibrational density of states pattern that we assign to both Fe−CO stretching modes [ν(Fe−CO)] and Fe−CO bending modes [δ(Fe−CO)], which are generated by two pairs of *cis*-CO ligands in inequivalent geometries. Similar patterns of ν(Fe−CO) stretches and δ(Fe−CO) bends were observed from 450 to 700 cm^{-1} for the Hmd hydrogenase as well as a *cis*-$(CO)_2$ ligated model complex, $Fe(S_2C_2H_4)(CO)_2(PMe_3)_2$.[24] It is known that there are significant differences in the dynamics of Fe−CO and Fe−CN moieties. For example, strong back-bonding in the Fe−CO moiety favors a linear Fe−C−O geometry and pushes the δ(Fe−CO) bends to higher frequencies than the ν(Fe−CO) stretches.[46] Our DFT calculations for the model complex support this finding (Supporting Information). Specifically, the 512 and 558 cm^{-1} ν(Fe−CO) bands are mainly from symmetric and asymmetric stretching motions, respectively, while the weak 584 cm^{-1} shoulder and strong 637 cm^{-1} band are mainly from in-plane and out-of-plane δ(Fe−CO) bending motions, respectively.

Turning to the ^{57}Fe PVDOS for the CpI$^{[^{57}Fe]H}$ hydrogenase (Figure 3), we can see a complex pattern of at least nine bands from 390 to 700 cm^{-1}, a region in which very little intensity is observed for either [4Fe-4S] or [2Fe-2S] clusters.[25,45] In the higher-energy portion (500−700 cm^{-1}), strong bands are shown at 528, 560, 585, and 604 cm^{-1}. On the basis of our analysis for the model compound, we assign these four strong bands as Fe−CO vibrations. We further propose the assignment of the 528 and 560 cm^{-1} peaks as mainly ν(Fe−CO) stretches, and the 585 and 604 cm^{-1} pair of peaks as mainly δ(Fe−CO) bends. Contrary to the Fe−CO moieties, weak back-bonding interactions exist with the Fe−CN moieties, resulting in a more nuanced situation in which either Fe−CN bond stretching or bending motions can be at the higher frequency, and in which there is likely extensive mixing.[47] Therefore, in the lower-energy portion of the 390−700 cm^{-1} region for the CpI$^{[^{57}Fe]}$ hydrogenase, we assign the two bands at 425 and 454 cm^{-1} as either ν(Fe−CN) stretches or δ(Fe−CN) bends. Relatively weaker bands are present from 460 to 510 cm^{-1} as well as from 610 to 670 cm^{-1}, and additional studies will help further characterize these possible Fe−CO and Fe−CN features.

EPR Spectroscopy. The iron analysis and NRVS data clearly indicate that the CpI$^{[^{57}Fe]H}$ hydrogenase has two ^{57}Fe-enriched Fe−S clusters, one of which is the $[2Fe]_H$ subcluster. A key question is whether the second ^{57}Fe−S cluster is the $[4Fe\text{-}4S]_H$ subcluster or one of the F-domain accessory clusters. EPR spectroscopy offers a route for characterizing the ^{57}Fe content within the H-cluster by quantifying the amount of broadening associated with the H_{ox} signal. It has been shown that this broadening arises from ^{57}Fe hyperfine interactions and increases with the number of ^{57}Fe nuclei in the six-iron H-cluster.[48] Considering that we already established the presence of an ^{57}Fe-labeled $[2Fe]_H$ subcluster from NRVS, we then used CW EPR to determine if the $[4Fe\text{-}4S]_H$ cluster associated with the CpI$^{[^{57}Fe]H}$ hydrogenase was the second Fe−S cluster labeled with ^{57}Fe nuclei.

Because the anaerobically purified CpI$^{[^{57}Fe]H}$ was prepared under a H_2 atmosphere (97% N_2 and 3% H_2), the NRVS sample was a mixture of both oxidized and H_2-reduced enzyme (Supporting Information, Figure S5). Following the NRVS experiments, the CpI$^{[^{57}Fe]H}$ sample was thawed, diluted, and treated with excess thionin acetate under a 100% N_2 atmosphere. This generated a completely oxidized hydrogenase sample with an $S = {}^1/_2$ rhombic signal (Figure 4, inset; g_1 = 2.100, g_2 = 2.042, and g_3 = 2.002) nearly identical to the H_{ox} spectrum for CpI activated *in vitro* using natural abundance Fe (CpI$^{[^{56}Fe]H}$) and for wild-type CpI produced in the native organism.[49,50] The main difference is that, as expected, the lines in the H_{ox} spectrum for the CpI$^{[^{57}Fe]H}$ hydrogenase were broader as a result of the hyperfine couplings that derive from the integrated ^{57}Fe nuclei. Specifically, the half-width at half-height (HWHH) at the g_1 tensor is 0.58 mT (Figure 4). On the basis of previous EPR spectroscopy of the *Desulfovibrio desulfuricans* [FeFe] hydrogenase,[48] this amount of broadening indicates that the CpI$^{[^{57}Fe]H}$ contains an H-cluster with approximately two ^{57}Fe nuclei. These results suggest that CpI$^{[^{57}Fe]H}$ hydrogenase has an H-cluster in which the $[2Fe]_H$

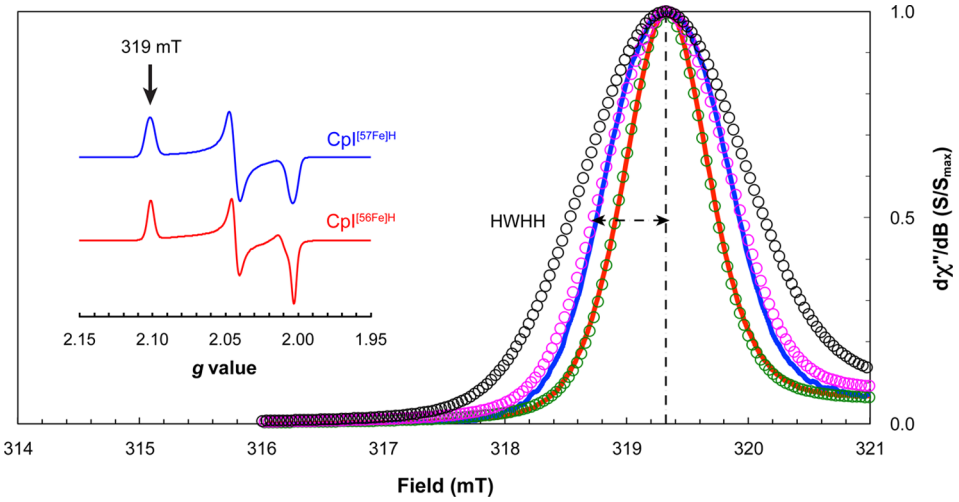

Figure 4. X-Band CW EPR spectroscopy of the CpI hydrogenase. Spectra near the g_1 tensor of the H_{ox} signal (g_1 = 2.101; ~319 mT) were measured at 50 K and 50 μW for CpI$^{[^{56}Fe]H}$ (red) and CpI$^{[^{57}Fe]H}$ (blue) following oxidation with excess thionin acetate. Simulations for the H_{ox} signal around 319 mT include hyperfine interactions from zero ^{57}Fe nuclei (green circles), two ^{57}Fe nuclei (magenta circles), and six ^{57}Fe nuclei (black circles), as determined using the $A_1{}^{ox}$ and $A_2{}^{ox}$ hyperfine values from the *D. desulfuricans* HydA hydrogenase.[48] Dashed lines are shown for the half-width at half-height (HWHH) for the CpI$^{[^{57}Fe]H}$ sample. The spectra shown in the inset represent the full H_{ox} signal for each hydrogenase sample as measured at 15 K and 62 μW.

dx.doi.org/10.1021/bi301336r | *Biochemistry* 2013, 52, 818−826

subcluster is enriched with ^{57}Fe, whereas the $[4Fe\text{-}4S]_H$ subcluster contains natural abundance ^{56}Fe.

DISCUSSION

Enriching proteins with rare isotopes such as ^{13}C and ^{15}N commonly involves growing a microorganism on growth medium supplemented with a substrate containing the particular isotopic element.[48] For the case of labeling Fe−S clusters, exogenous ^{57}Fe can be added to the cell culture, and the host cell iron−sulfur cluster machinery will ubiquitously assemble ^{57}Fe−S clusters onto proteins that coordinate these metal centers. Nevertheless, global enrichment of a single protein is often undesirable if numerous isotopic nuclei will lead to confounding experimental results. Targeted isotopic enrichment is far more challenging and, ultimately, requires a method in which there is precise control over the biochemical process that involves the incorporation of the isotopic element.

In vitro systems offer unique opportunities to label proteins with a variety of non-natural or isotopic elements. For example, cell-free protein synthesis platforms can be used to incorporate amino acid isotopologs,[51,52] or even non-natural amino acids,[53] either globally or at selected sites within a polypeptide chain. However, unlike protein translation with its generalized machinery, post-translational processes commonly require specialized accessory proteins. Incorporating isotopically enriched metal clusters and other cofactors during a particular post-translational reaction likely necessitates an *in vitro* system in which the biochemical pathway has been reconstituted. Interestingly, we have developed a cell-free system in which the $[2Fe]_H$ subcluster can be synthesized and transferred to the hydrogenase in a reaction sequence that is distinctly separated from protein translation.[15]

As we have shown in this study, the precise control of both the maturases and the low-molecular weight substrates allowed us to design a cell-free reaction mixture that synthesized an ^{57}Fe-labeled $[2Fe]_H$ subcluster onto a hydrogenase apoprotein containing ^{56}Fe-labeled Fe−S clusters. We then utilized two spectroscopic techniques to probe and characterize the [FeFe] hydrogenase, and our results confirm the incorporation of ^{57}Fe into the enzyme's active site metal center. Specifically, we used NRVS to assign various normal modes for the hydrogenase by comparing the ^{57}Fe vibrational density of states to those of a [4Fe-4S] ferredoxin and a $[2Fe]_H$ subcluster model complex, revealing ^{57}Fe−CO and ^{57}Fe−CN moieties associated with the CpI enzyme (Figure 3) and confirming the cell-free assembly of an ^{57}Fe-enriched $[2Fe]_H$ catalytic subunit. By complementing the NRVS with EPR spectroscopy, we observed distinct broadening of the H_{ox} EPR signal for the $CpI^{[^{57}Fe]H}$ enzyme (Figure 4), which further shows that the hydrogenase contains an ^{57}Fe-labeled $[2Fe]_H$ subcluster.

The region in which we would expect Fe−CO and Fe−CN vibrational modes (400−700 cm^{-1}) is distinct from the region with Fe−S vibrational modes. This fortuitous circumstance simplifies the characterization of modes that come from the non-protein ligands of the H-cluster. The clear observation of Fe−CO and Fe−CN normal modes in this work demonstrates that NRVS is another capable approach to studying [FeFe] hydrogenases. More interestingly, our results establish precedence for future NRVS studies for probing bound hydrides (i.e., Fe−H and Fe−^{2}H modes). This will be crucial for understanding the mechanism of hydrogen activation and for developing synthetic catalysts that function like the H-cluster. In addition, spectral simulations along with isotopic labeling of the $[2Fe]_H$ subcluster using ^{13}C, ^{15}N, ^{18}O, and ^{36}S could help definitively assign the Fe−S, Fe−CO, and Fe−CN normal modes. The *in vitro* system used in this work has proven to be effective for the synthesis of the $[2Fe]_H$ subcluster with isotopically labeled substituents.[15] In our previous study, we demonstrated the cell-free production of ^{13}CO and $^{13}CN^-/^{13}C^{15}N^-$ ligands from various tyrosine isotopologs, conclusively showing that all five CO and CN^- adducts derive from this amino acid.

Our general characterization of the Fe−CO modes for the $CpI^{[^{57}Fe]H}$ hydrogenase and the model complex is supported by our DFT calculations for the model compound as well as from previous NRVS of the Hmd hydrogenase where multiple peaks from 480 to 700 cm^{-1} were attributed to Fe−CO modes.[24] With respect to the $[2Fe]_H$ subcluster CN^- ligands, we have assigned peaks from 410 to 450 cm^{-1} to Fe−CN vibrational modes. In reasonable agreement with our assignments, and on the basis of isotope shifts along with normal mode analysis for the model complex, Fiedler and Brunold assigned a resonance Raman band at 390 cm^{-1} to a δ(Fe−CN) bending mode, and bands at 432 and 450 cm^{-1} to ν(Fe−CN) stretching modes.[54] We also note that the $[2Fe]_H$ subcluster Fe−CN modes have modestly lower frequencies than those observed in spectroscopic studies of heme-related Fe−CN moieties. For example, ferrous cytochrome a_3 oxidases have Fe^{II}−CN modes with energies from 470 to 510 cm^{-1}.[47] Conversely, the $[^{57}Fe_2(S_2C_3H_6)(CN)_2(CO)_4]^{2-}$ model compound, which is an Fe^I/Fe^I complex, has Fe^I−CN modes at lower energies from 410 to 450 cm^{-1}. With regard to the electronic structures of the $[2Fe]_H$ subcluster, conflicting results have been reported. Mössbauer studies have indicated the electronic structures to be Fe_p^{II}/Fe_d^{III} (H_{ox}) and Fe_p^{II}/Fe_d^{II} (H_{red}).[55] EPR and FTIR spectroscopy have pointed to structures of Fe_p^{I}/Fe_d^{II} (H_{ox}) and Fe_p^{I}/Fe_d^{I} (H_{red}).[48] In this study, the NRVS spectrum for the $CpI^{[^{57}Fe]H}$ hydrogenase shows peaks at 425 and 454 cm^{-1}, which are likely attributed to Fe^I−CN modes, supporting the Fe_p^{I}/Fe_d^{II} (H_{ox}) and Fe_p^{I}/Fe_d^{I} (H_{red}) electronic structures assigned by Silakov and co-workers.

Analysis of the vibrational density of states within the Fe−S region (Figure 2) suggests that the $CpI^{[^{57}Fe]H}$ hydrogenase has an additional ^{57}Fe−S cluster besides the $[2Fe]_H$ subcluster that was assembled during the *in vitro* activation reaction. The three peaks at 282, 353, and 382 cm^{-1} together with NRVS data for the oxidized ferredoxin indicate the presence of a $[4Fe\text{-}4S]^{2+}$ cluster. We also compared the relative amounts of total NRVS intensity within the Fe−S and Fe−CO/Fe−CN regions (Supporting Information, Table S2). Roughly twice as much intensity is derived from ^{57}Fe−S modes for $CpI^{[^{57}Fe]H}$ relative to that from the ^{57}Fe−CO/^{57}Fe−CN modes. This result, together with the difference in the iron content between the apoprotein (∼13 Fe atoms per CpI) and the holoenzyme (∼18 Fe atoms per CpI), further supports our assignment of an ^{57}Fe-enriched [4Fe-4S] cluster associated with the $CpI^{[^{57}Fe]H}$ hydrogenase.

We speculated that the ^{57}Fe-labeled [4Fe-4S] cluster might be the companion $[4Fe\text{-}4S]_H$ subcluster rather than one of the three accessory [4Fe-4S] clusters. As previously stated, EPR spectroscopy provides a way to probe as well as to quantitate protein-bound ^{57}Fe atoms based on the hyperfine interactions resulting from these magnetic nuclei. When the CpI hydrogenase is in the oxidized and active state, the H-cluster (H_{ox}) is EPR-active, whereas the accessory Fe−S clusters are EPR-silent. This fortunate situation means that the entire amount of line broadening associated with the H_{ox} signal that we observed results only from

dx.doi.org/10.1021/bi301336r | *Biochemistry* 2013, 52, 818−826

^{57}Fe nuclei within the H-cluster. Based on previous results by Silakov and co-workers, the amount of broadening for CpI$^{[^{57}Fe]H}$ (HWHH of 0.58 mT) suggests that the H-cluster has two ^{57}Fe nuclei rather than the expected six if the H-cluster was completely enriched.[48] This finding clearly indicates that only the $[2Fe]_H$ subcluster is ^{57}Fe-labeled, whereas the $[4Fe\text{-}4S]_H$ subcluster is not enriched with ^{57}Fe. It is noteworthy that in this study, the maturation reaction mixtures for producing the CpI$^{[^{57}Fe]H}$ samples contained ^{57}Fe-enriched Hyd maturases as well as exogenously added ^{57}Fe. Therefore, the $[2Fe]_H$ subcluster is presumably homogeneously enriched with ^{57}Fe, and all ^{56}Fe-enriched Fe−S clusters associated with CpI$^{[^{57}Fe]H}$ were likely assembled *in vivo* during heterologous expression of the hydrogenase apoprotein. It follows that the $[4Fe\text{-}4S]_H$ subcluster was not synthesized *in vitro* during hydrogenase maturation.

By illustrating that the CpI$^{[^{57}Fe]H}$ hydrogenase retained an ^{56}Fe-labeled $[4Fe\text{-}4S]_H$ during the ^{57}Fe-enriched cell-free maturation reaction, we provide unequivocal evidence that supports a stepwise maturation sequence postulated by Mulder and co-workers.[18] In their study, X-ray crystallography of the *Chlamydomonas reinhardtii* HydA1 hydrogenase revealed a cationic channel associated with the $[4Fe\text{-}4S]_H$-containing apoprotein. The authors suggested that HydF transfers the $[2Fe]_H$ subcluster through the channel to the H-domain, which is followed by a conformational change that leads to an active hydrogenase devoid of the channel.

It could be expected that the enclosed nature of the H-domain would necessitate the assembly of the $[4Fe\text{-}4S]_H$ subcluster before the activation reaction, perhaps prior to or during protein folding. In contrast to the H-cluster, the N-terminal domain ancillary clusters are more accessible to the intracellular environment. It seems possible that one of the iron centers is fairly unstable, and thus labile before or during the purification process. The similarities and differences among the three F-domain accessory [4Fe-4S] clusters are not well characterized, and NRVS of multiple protein variants would be required to elucidate which [4Fe-4S] cluster is labeled with ^{57}Fe.

In summary, we have used NRVS to measure the ^{57}Fe-based vibrational density of states of the [FeFe] hydrogenase from *C. pasteurianum* as well as a model complex resembling the $[2Fe]_H$ subcluster. This report not only presents the first NRVS of [FeFe] hydrogenases but also, to the best of our knowledge, provides the first example of isotopically enriching a specific protein-bound metal cluster among several other clusters for NRVS. Because the CpI enzyme contains multiple Fe−S centers, selective labeling of the $[2Fe]_H$ subcluster with ^{57}Fe substantially improved the ^{57}Fe PVDOS intensities within the Fe−CO/Fe−CN region, thus facilitating a more facile characterization of these relatively weak vibrational modes. Such increased signal intensity within the higher-energy region will be crucial for probing another interesting H-cluster feature, the Fe−H vibration. Finally, the combination of NRVS with EPR spectroscopy allowed us to demonstrate the separate insertion of the $[2Fe]_H$ and $[4Fe\text{-}4S]_H$ subclusters. In this way, we have shown how cell-free biochemistry along with advanced spectroscopic techniques is a powerful combination capable of answering fundamental questions about the biological chemistry of a complex metalloenzyme and its unique maturation pathway.

■ ASSOCIATED CONTENT

Supporting Information

Synthesis details, DFT calculations, and IR spectroscopy of the $(Et_4N)_2[^{57}Fe_2(S_2C_3H_6)(CN)_2(CO)_4]$ model compound; figure comparing the full NRVS spectra for two CpI$^{[^{57}Fe]H}$ samples, two model compounds (^{12}CN-labeled and ^{13}CN-labeled), and two *Pf* D14C Fd samples (oxidized and reduced); table with percentages of total ^{57}Fe intensity within the Fe−S and Fe−CO/Fe−CN regions; and EPR spectra of ^{57}Fe-enriched CpI (pre- and post-NRVS) and ^{56}Fe-enriched CpI. This material is available free of charge via the Internet at http://pubs.acs.org.

■ AUTHOR INFORMATION

Corresponding Author

*Phone: (650) 823-0557. E-mail: spjcramer@ucdavis.edu.

Present Addresses

∞Present Address: Department of Chemistry, the Pennsylvania State University, University Park, Pennsylvania 16802, United States.

Funding

This work was funded by the National Institutes of Health (GM-65440, S.P.C.); the U.S. Department of Energy, Office of Biological and Environmental Research; and the U.S. Department of Energy, Office of Basic Energy Sciences (DE-FG02-09ER46632, J.R.S. and S.P.C.). Research at SPring-8 was funded by proposals 2010B0032 (S.P.C.) and 2012A0032 (S.P.C.), and research at the Advanced Photon Source was supported by the U.S. Department of Energy, Office of Basic Energy Sciences.

Notes

The authors declare no competing financial interest.

■ ACKNOWLEDGMENTS

We thank Thomas Rauchfuss and Saeed Kamali for insightful discussions pertaining to the manuscript. We also thank Matt C. Smith and Yuming Xiao for their assistance during the NRVS measurements of the model complex.

■ ABBREVIATIONS

NRVS, nuclear resonance vibrational spectroscopy; PVDOS, partial vibrational density of states; EPR, electron paramagnetic resonance; IR, infrared; RR, resonance Raman; DFT, density functional theory; *Pf* D14C Fd, *P. furiosus* [4Fe-4S] ferredoxin D14C variant; CpI, *C. pasteurianum* HydA [FeFe] hydrogenase; CO, carbon monoxide; CN, cyanide; DTMX, H-cluster bridging ligand that is either dithiomethylamine (DTMA) or dithiomethylether (DTMO); GTP, guanosine 5′-triphosphate; DTT, dithiothreitol.

■ REFERENCES

(1) Ghirardi, M. L., Dubini, A., Yu, J., and Maness, P.-C. (2009) Photobiological hydrogen-producing systems. *Chem. Soc. Rev. 38*, 52−61.

(2) Vignais, P. M., and Billoud, B. (2007) Occurrence, classification, and biological function of hydrogenases: An overview. *Chem. Rev. 107*, 4206−4272.

(3) Martin, W., and Müller, M. (1998) The hydrogen hypothesis for the first eukaryote. *Nature 392*, 37−41.

(4) Kruse, O., and Hankamer, B. (2010) Microalgal hydrogen production. *Curr. Opin. Biotechnol. 21*, 1−6.

(5) Zhang, Y.-H. P., Evans, B. R., Mielenz, J. R., Hopkins, R. C., and Adams, M. W. W. (2007) High-yield hydrogen production from starch and water by a synthetic enzymatic pathway. *PLoS ONE 2*, e456.

(6) Hambourger, M., Gervaldo, M., Svedruzic, D., King, P. W., Gust, D., Ghirardi, M., Moore, A. L., and Moore, T. A. (2008) [FeFe]-hydrogenase-catalyzed H2 production in a photoelectrochemical biofuel cell. *J. Am. Chem. Soc. 130*, 2015−2022.
(7) Iwuchukwu, I. J., Vaughn, M., Myers, N., O'Neill, H., Frymier, P., and Bruce, B. D. (2010) Self-organized photosynthetic nanoparticle for cell-free hydrogen production. *Nat. Nanotechnol. 5*, 73−79.
(8) Le Goff, A., Artero, V., Jousselme, B., Tran, P. D., Guillet, N., Métayé, R., Fihri, A., Palacin, S., and Fontecave, M. (2009) From hydrogenases to noble metal-free catalytic nanomaterials for H2 production and uptake. *Science 326*, 1384−1387.
(9) Tard, C., and Pickett, C. J. (2009) Structural and functional analogues of the active sites of the [Fe]-, [NiFe]-, and [FeFe]-hydrogenases. *Chem. Rev. 109*, 2245−2274.
(10) Nicolet, Y., Piras, C., Legrand, P., Hatchikian, C. E., and Fontecilla-Camps, J. C. (1999) *Desulfovibrio desulfuricans* iron hydrogenase: The structure shows unusual coordination to an active site Fe binuclear center. *Structure 7*, 13−23.
(11) Peters, J. W., Lanzilotta, W. N., Lemon, B. J., and Seefeldt, L. C. (1998) X-ray crystal structure of the Fe-only hydrogenase (CpI) from *Clostridium pasteurianum* to 1.8 angstrom resolution. *Science 282*, 1853−1858.
(12) Mulder, D. W., Shepard, E. M., Meuser, J. E., Joshi, N., King, P. W., Posewitz, M. C., Broderick, J. B., and Peters, J. W. (2011) Insights into [FeFe]-hydrogenase structure, mechanism, and maturation. *Structure 19*, 1038−1052.
(13) Posewitz, M. C., King, P. W., Smolinski, S. L., Zhang, L., Seibert, M., and Ghirardi, M. L. (2004) Discovery of two novel radical S-adenosylmethionine proteins required for the assembly of an active [Fe] hydrogenase. *J. Biol. Chem. 279*, 25711−25720.
(14) Kuchenreuther, J. M., Britt, R. D., and Swartz, J. R. (2012) New insights into [FeFe] hydrogenase activation and maturase function. *PLoS ONE 7*, e45850.
(15) Kuchenreuther, J. M., George, S. J., Grady-Smith, C. S., Cramer, S. P., and Swartz, J. R. (2011) Cell-free H-cluster synthesis and [FeFe] hydrogenase activation: All five CO and CN^- ligands derive from tyrosine. *PLoS ONE 6*, e20346.
(16) Kuchenreuther, J. M., Stapleton, J. A., and Swartz, J. R. (2009) Tyrosine, cysteine, and S-adenosyl methionine stimulate *in vitro* [FeFe] hydrogenase activation. *PLoS ONE 4*, e7565.
(17) McGlynn, S. E., Shepard, E. M., Winslow, M. A., Naumov, A. V., Duschene, K. S., Posewitz, M. C., Broderick, W. E., Broderick, J. B., and Peters, J. W. (2008) HydF as a scaffold protein in [FeFe] hydrogenase H-cluster biosynthesis. *FEBS Lett. 582*, 2183−2187.
(18) Mulder, D. W., Boyd, E. S., Sarma, R., Lange, R. K., Endrizzi, J. A., Broderick, J. B., and Peters, J. W. (2010) Stepwise [FeFe]-hydrogenase H-cluster assembly revealed in the structure of HydA(ΔEFG). *Nature 465*, 248−252.
(19) Chen, Z., Lemon, B. J., Huang, S., Swartz, D. J., Peters, J. W., and Bagley, K. A. (2002) Infrared studies of the CO-inhibited form of the Fe-only hydrogenase from *Clostridium pasteurianum* I: Examination of its light sensitivity at cryogenic temperatures. *Biochemistry 41*, 2036−2043.
(20) Lubitz, W., Reijerse, E., and van Gastel, M. (2007) [NiFe] and [FeFe] hydrogenases studied by advanced magnetic resonance techniques. *Chem. Rev. 107*, 4331−4365.
(21) Roseboom, W., de Lacey, A. L., Fernandez, V. M., Hatchikian, E. C., and Albracht, S. P. J. (2006) The active site of the [FeFe]-hydrogenase from *Desulfovibrio desulfuricans*. II. Redox properties, light sensitivity and CO-ligand exchange as observed by infrared spectroscopy. *J. Biol. Inorg. Chem. 11*, 102−118.
(22) Bruschi, M., Greco, C., Kaukonen, M., Fantucci, P., Ryde, U., and De Gioia, L. (2009) Influence of the [2Fe]H subcluster environment on the properties of key intermediates in the catalytic cycle of [FeFe] hydrogenases: Hints for the rational design of synthetic catalysts. *Angew. Chem., Int. Ed. 48*, 3503−3506.
(23) Bingham, A. S., Smith, P. R., and Swartz, J. R. (2012) Evolution of an [FeFe] hydrogenase with decreased oxygen sensitivity. *Int. J. Hydrogen Energy 37*, 2965−2976.
(24) Guo, Y., Wang, H., Xiao, Y., Vogt, S., Thauer, R. K., Shima, S., Volkers, P. I., Rauchfuss, T. B., Pelmenschikov, V., Case, D. A., Alp, E. E., Sturhahn, W., Yoda, Y., and Cramer, S. P. (2008) Characterization of the Fe site in iron-sulfur cluster-free hydrogenase (Hmd) and of a model compound via nuclear resonance vibrational spectroscopy (NRVS). *Inorg. Chem. 47*, 3969−3977.
(25) Mitra, D., Pelmenschikov, V., Guo, Y., Case, D. A., Wang, H., Dong, W., Tan, M.-L., Ichiye, T., Jenney, F. E., Adams, M. W. W., Yoda, Y., Zhao, J., and Cramer, S. P. (2011) Dynamics of the [4Fe-4S] cluster in *Pyrococcus furiosus* D14C ferredoxin via nuclear resonance vibrational and resonance Raman spectroscopies, force field simulations, and density functional theory calculations. *Biochemistry 50*, 5220−5235.
(26) Xiao, Y., Fisher, K., Smith, M. C., Newton, W. E., Case, D. A., George, S. J., Wang, H., Sturhahn, W., Alp, E. E., Zhao, J., Yoda, Y., and Cramer, S. P. (2006) How nitrogenase shakes: Initial information about P-cluster and FeMo-cofactor normal modes from nuclear resonance vibrational spectroscopy (NRVS). *J. Am. Chem. Soc. 128*, 7608−7612.
(27) Alp, E., Sturhahn, W., Toellner, T., Zhao, J., Hu, M., and Brown, D. (2002) Vibrational Dynamics Studies by Nuclear Resonant Inelastic X-Ray Scattering. *Hyperfine Interact. 144−145*, 3−20.
(28) Petrenko, T., Sturhahn, W., and Neese, F. (2007) First-principles calculation of nuclear resonance vibrational spectra. *Hyperfine Interact. 175*, 165−174.
(29) Scheidt, W. R., Durbin, S. M., and Sage, J. T. (2005) Nuclear resonance vibrational spectroscopy—NRVS. *J. Inorg. Biochem. 99*, 60−71.
(30) Sturhahn, W. (2004) Nuclear resonant spectroscopy. *J. Phys.: Condens. Matter 16*, S497.
(31) Nakamoto, K. (1997) *Infrared and Raman Spectra of Inorganic and Coordination Compounds: Theory and applications in inorganic chemistry (Part A)*, 5th ed., Wiley-Interscience, New York.
(32) Leu, B. M., Zgierski, M. Z., Wyllie, G. R. A., Scheidt, W. R., Sturhahn, W., Alp, E. E., Durbin, S. M., and Sage, J. T. (2004) Quantitative Vibrational Dynamics of Iron in Nitrosyl Porphyrins. *J. Am. Chem. Soc. 126*, 4211−4227.
(33) Sage, J., Paxson, C., Wyllie, G. R. A., Sturhahn, W., Durbin, S. M., Champion, P. M., Alp, E. E., and Scheidt, W. R. (2001) Nuclear resonance vibrational spectroscopy of a protein active-site mimic. *J. Phys.: Condens. Matter 13*, 7707−7722.
(34) Sturhahn, W., Toellner, T. S., Alp, E. E., Zhang, X., Ando, M., Yoda, Y., Kikuta, S., Seto, M., Kimball, C. W., and Dabrowski, B. (1995) Phonon density of states measured by inelastic nuclear resonant scattering. *Phys. Rev. Lett. 74*, 3832−3835.
(35) Kuchenreuther, J. M., Grady-Smith, C. S., Bingham, A. S., George, S. J., Cramer, S. P., and Swartz, J. R. (2010) High-yield expression of heterologous [FeFe] hydrogenases in *Escherichia coli*. *PLoS ONE 5*, e15491.
(36) Fish, W. W. (1988) Rapid colorimetric micromethod for the quantitation of complexed iron in biological samples. *Methods Enzymol. 158*, 357−364.
(37) Czech, I., Silakov, A., Lubitz, W., and Happe, T. (2009) The [FeFe]-hydrogenase maturase HydF from *Clostridium acetobutylicum* contains a CO and CN^- ligated iron cofactor. *FEBS Lett. 584*, 638−642.
(38) Bradford, M. M. (1976) A rapid and sensitive method for the quantitation of microgram quantities of protein utilizing the principle of protein-dye binding. *Anal. Biochem. 72*, 248−254.
(39) Adams, M. W., Eccleston, E., and Howard, J. B. (1989) Iron-sulfur clusters of hydrogenase I and hydrogenase II of *Clostridium pasteurianum*. *Proc. Natl. Acad. Sci. U.S.A. 86*, 4932−4936.
(40) Sturhahn, W. (2000) CONUSS and PHOENIX: Evaluation of nuclear resonant scattering data. *Hyperfine Interact. 125*, 149−172.
(41) Yoda, Y., Yabashi, M., Izumi, K., Zhang, X. W., Kishimoto, S., Kitao, S., Seto, M., Mitsui, T., Harami, T., Imai, Y., and Kikuta, S. (2001) Nuclear resonant scattering beamline at SPring-8. *Nucl. Instrum. Methods Phys. Res., Sect. A 467*, 715−718.
(42) Toellner, T. (2000) Monochromatization of synchrotron radiation for nuclear resonant scattering experiments. *Hyperfine Interact. 125*, 3−28.

(43) Stoll, S., and Schweiger, A. (2006) EasySpin, a comprehensive software package for spectral simulation and analysis in EPR. *J. Magn. Reson. 178*, 42−55.
(44) Shepard, E. M., McGlynn, S. E., Bueling, A. L., Grady-Smith, C. S., George, S. J., Winslow, M. A., Cramer, S. P., Peters, J. W., and Broderick, J. B. (2010) Synthesis of the 2Fe subcluster of the [FeFe]-hydrogenase H cluster on the HydF scaffold. *Proc. Natl. Acad. Sci. U.S.A. 107*, 10448−10453.
(45) Xiao, Y., Tan, M.-L., Ichiye, T., Wang, H., Guo, Y., Smith, M. C., Meyer, J., Sturhahn, W., Alp, E. E., Zhao, J., Yoda, Y., and Cramer, S. P. (2008) Dynamics of *Rhodobacter capsulatus* [2Fe-2S] ferredoxin VI and *Aquifex aeolicus* ferredoxin 5 via nuclear resonance vibrational spectroscopy (NRVS) and resonance Raman spectroscopy. *Biochemistry 47*, 6612−6627.
(46) Nakamoto, K. (1997) *Infrared and Raman Spectra of Inorganic and Coordination Compounds: Applications in coordination, organometallic, and bioinorganic chemistry (Part B)*, 5th ed., Wiley-Interscience, New York.
(47) Kim, Y., Babcock, G. T., Surerus, K. K., Fee, J. A., Dyer, R. B., Woodruff, W. H., and Oertling, W. A. (1998) Cyanide binding and active site structure in heme-copper oxidases: Normal coordinate analysis of iron-cyanide vibrations of a3(2+)CN- complexes of cytochromes ba3 and aa3. *Biospectroscopy 4*, 1−15.
(48) Silakov, A., Reijerse, E. J., Albracht, S. P. J., Hatchikian, E. C., and Lubitz, W. (2007) The electronic structure of the H-cluster in the [FeFe]-hydrogenase from *Desulfovibrio desulfuricans*: A Q-band ^{57}Fe-ENDOR and HYSCORE study. *J. Am. Chem. Soc. 129*, 11447−11458.
(49) Adams, M. W. (1987) The mechanisms of H_2 activation and CO binding by hydrogenase I and hydrogenase II of *Clostridium pasteurianum*. *J. Biol. Chem. 262*, 15054−15061.
(50) Chen, J.-S., and Mortenson, L. E. (1976) in *Iron and Copper Proteins* (Yasunobu, K. T., Mower, H. F., and Hayaishi, O., Eds.) pp 68−82, Plenum Press, New York.
(51) Boyer, M. E., Stapleton, J. A., Kuchenreuther, J. M., Wang, C.-W., and Swartz, J. R. (2008) Cell-free synthesis and maturation of [FeFe] hydrogenases. *Biotechnol. Bioeng. 99*, 59−67.
(52) Boyer, M. E., Wang, C.-W., and Swartz, J. R. (2006) Simultaneous expression and maturation of the iron-sulfur protein ferredoxin in a cell-free system. *Biotechnol. Bioeng. 94*, 128−138.
(53) Patel, K. G., Ng, P. P., Kuo, C. C., Levy, S., Levy, R., and Swartz, J. R. (2009) Cell-free production of *Gaussia princeps* luciferase−antibody fragment bioconjugates for ex vivo detection of tumor cells. *Biochem. Biophys. Res. Commun. 390*, 971−976.
(54) Fiedler, A. T., and Brunold, T. C. (2005) Combined spectroscopic/computational study of binuclear Fe(I)-Fe(I) complexes: Implications for the fully-reduced active-site cluster of Fe-only hydrogenases. *Inorg. Chem. 44*, 1794−1809.
(55) Popescu, C., and Münck, E. (1999) Electronic structure of the H cluster in [Fe]-hydrogenases. *J. Am. Chem. Soc. 121*, 7877−7884.
(56) Pettersen, E. F., Goddard, T. D., Huang, C. C., Couch, G. S., Greenblatt, D. M., Meng, E. C., and Ferrin, T. E. (2004) UCSF Chimera: A visualization system for exploratory research and analysis. *J. Comput. Chem. 25*, 1605−1612.